Stem Cell Reports, Volume *1*

Supplemental Information

Long-Term Self-Renewal of Human ES/iPS-Derived Hepatoblast-like Cells on Human Laminin 111-Coated Dishes

Kazuo Takayama, Yasuhito Nagamoto, Natsumi Mimura, Katsuhisa Tashiro, Fuminori Sakurai, Masashi Tachibana, Takao Hayakawa, Kenji Kawabata, and Hiroyuki Mizuguchi

Supplemental figure 1

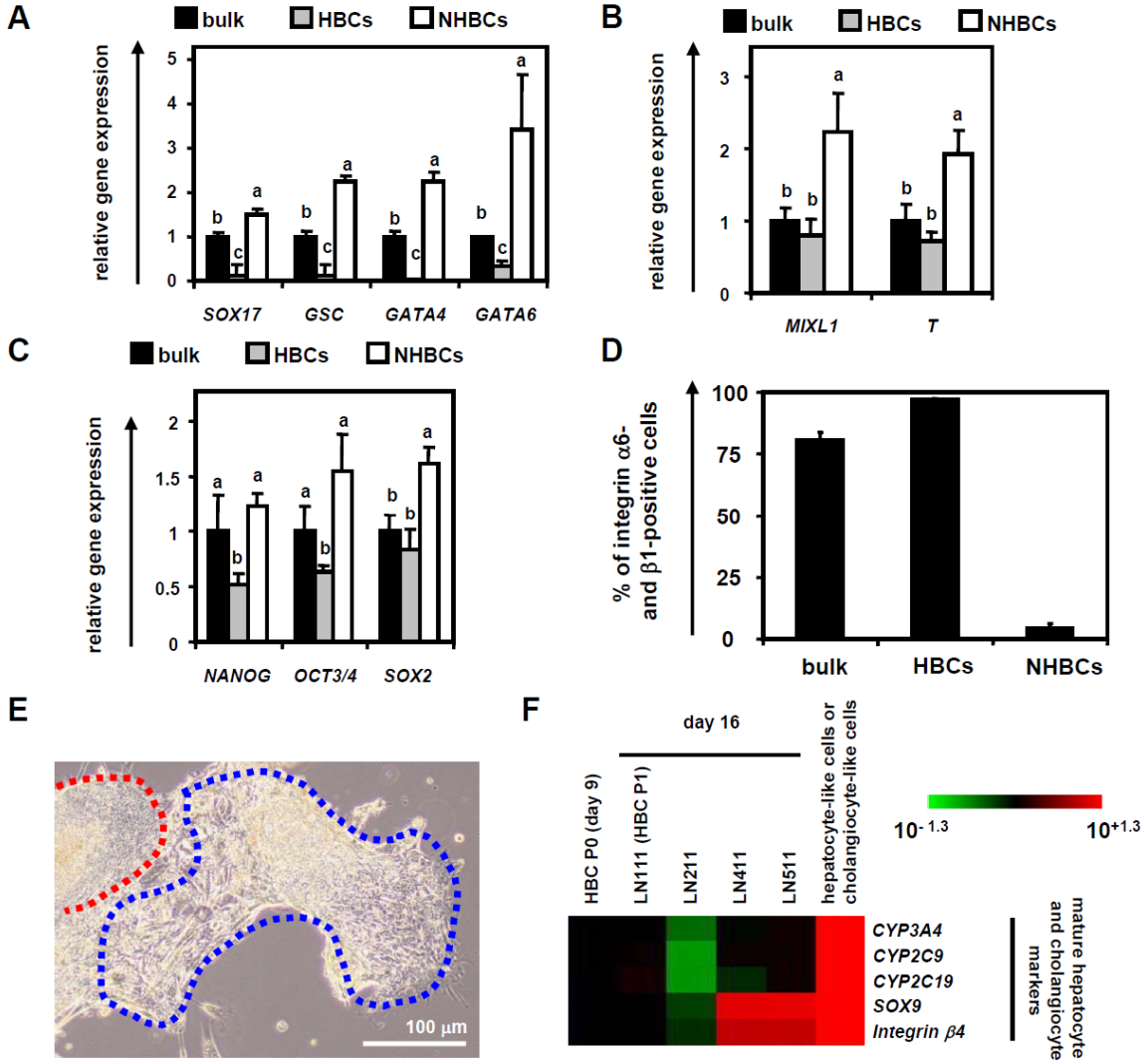

Figure S1. The characterization and purification of the hESC-derived HBCs, Related to Figure 1

(**A-C**) On day 9, the hESC (H9)-derived HBCs and NHBCs were manually picked up and pooled into groups, and the gene expression levels of (**A**) definitive endoderm markers (*SOX17*, *GSC*, *GATA4*, and *GATA6*), (**B**) mesendoderm markers (*MIXL1* and *T*), and (**C**) pluripotent markers (*NANOG*, *OCT3/4*, and *SOX2*) were measured by real-time RT-PCR. The gene expression in the human ESC-derived cells (day 9; bulk) was taken as 1.0. Data represent the mean ± SD from three independent experiments. Statistical significance was evaluated by ANOVA followed by Bonferroni post-hoc tests to compare three groups (bulk, HBCs, and NHBCs). Groups that do not share the same letter are significantly different from each other ($P<0.05$). (**D**) The percentage of both integrin α6 and β1-double positive

cells was measured by using FACS analysis. Data represent the mean ± SD from seven independent experiments. (**E**) The hESC -derived HBCs were manually picked up and passaged onto a LN111-coated dish, and then cultured for 3 days. Phase-contrast micrographs are shown. The cells indicated in red resembled human hepatic stem cells and the cells indicated in blue resembled human hepatoblasts (Schmelzer et al., 2007; Zhang et al., 2008). (**F**) The hESC-derived cells (day 9) were plated onto human LN111, 211, 411, or 511-coated dish. The gene expression levels of mature hepatocyte markers (*CYP3A4*, *2C9*, and *2C19*) or cholangiocyte markers (*SOX9* and *integrin β4*) were measured by real-time RT-PCR on day 16. The gene expression levels in the hESC-derived HBCs (the LN111-attached cells were collected at 15 min from plating) were taken as 1.0. Data represent the mean ± SD from three independent experiments. The gene expression levels of *SOX9* and *integrin β4* in the cells on LN411 or LN511 coated dishes were significantly different from other three groups (HBC P0, LN111, and LN211) based on analysis with one-way ANOVA followed by Bonferroni post-hoc tests ($P<0.05$).

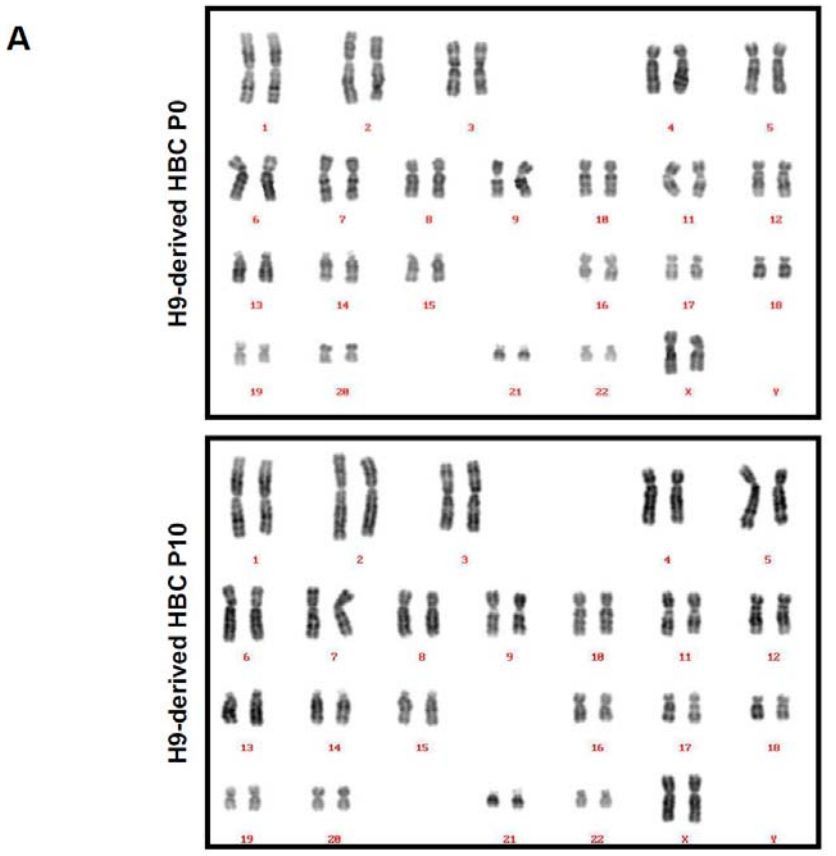
A
H9-derived HBC P0
H9-derived HBC P10
B
6 hr after passage on LN111
DAPI
HNF4α
MERGE
AFP
MERGE
C
7 days after passage on LN111
DAPI
ALB
MERGE
CK7
MERGE

Figure S2. Karyotype and colony formation capacity of the hESC-derived HBCs on a human LN111-coated dish, Related to Figure 3

(**A**) Karyotypes of hESC (H9)-derived HBC P0 and HBC P10 are shown, respectively. Chromosomal Q-band analyses showed that the human ESC (H9)-derived HBC P0 and P10 had a normal karyotype, indicating that the genetic stability of the HBCs was confirmed throughout the maintenance period. (**B**) The single hESC (H9)-derived HBC was plated in separate wells of a human LN111-coated 96-well plate. After 6 hr of plating, the expression of AFP (green) and HNF4α (red) were examined by immunohistochemistry. Nuclei were counterstained with DAPI (blue). Scale bar represents 20 μm. (**C**) After 7 days of plating, the expression of ALB (red) and CK7 (green) in hESC-derived HBC colony were examined by immunohistochemistry. Nuclei were counterstained with DAPI (blue). Scale bar represents 20 μm.

Supplemental figure 3

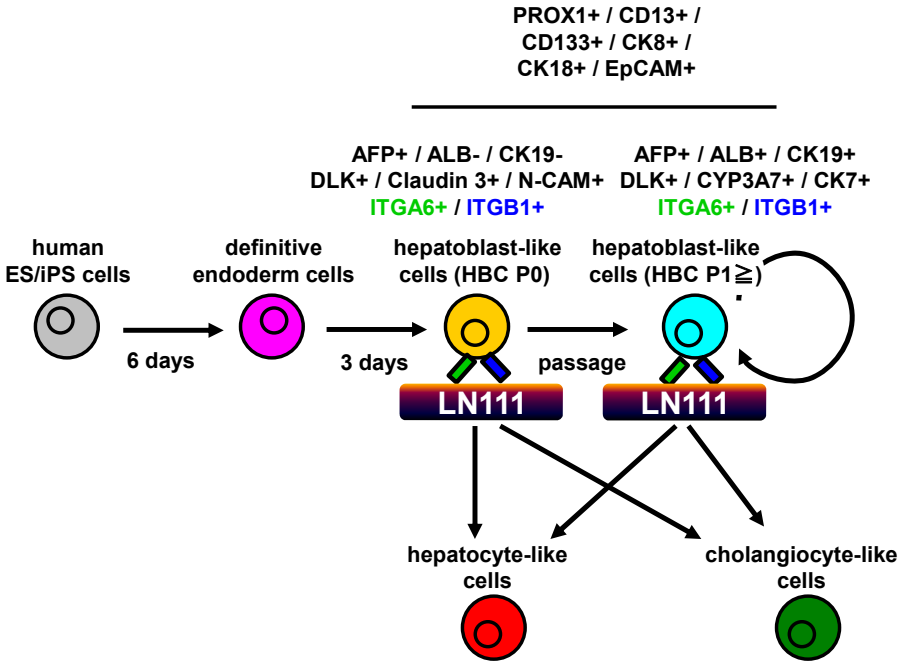

	HBC P0	HBC P1	HBC P10	HBC clone
	hPSC-derived cells (day 9) which attached to human LN111-coated dish	HBCs which were cultured on human LN111-coated dish for 7 days	HBCs that were passaged to human LN111-coated dish for 10 times	HBCs which were derived from single hPSC-derived HBC
differentiation capacity into hepatocyte and cholangiocyte	bipotent	bipotent	bipotent	bipotent
ability to integrate into liver parenchyma	+	not examined	+	not examined
average cell diameter	10 μm≦	10 μm≧	10 μm≧	10 μm≧
nucleus to to cytoplasmic raito	very high	intermediate	intermediate	intermediate
self-renewal	not succeeded	self-renewed on LN111	self-renewed on LN111	self-renewed on LN111

Figure S3. The characteristics of the hPSC-derived HBCs are summarized, Related to Figure 3

The hPSC-derived HBCs exhibited the ability to differentiate into both hepatic and biliary lineages. Long-term culture of HBCs derived from human pluripotent stem cells could be performed. The definitions of the hPSC-derived HBC P0, P1, P10, and clone in the present study are summarized.

Supplemental figure 4

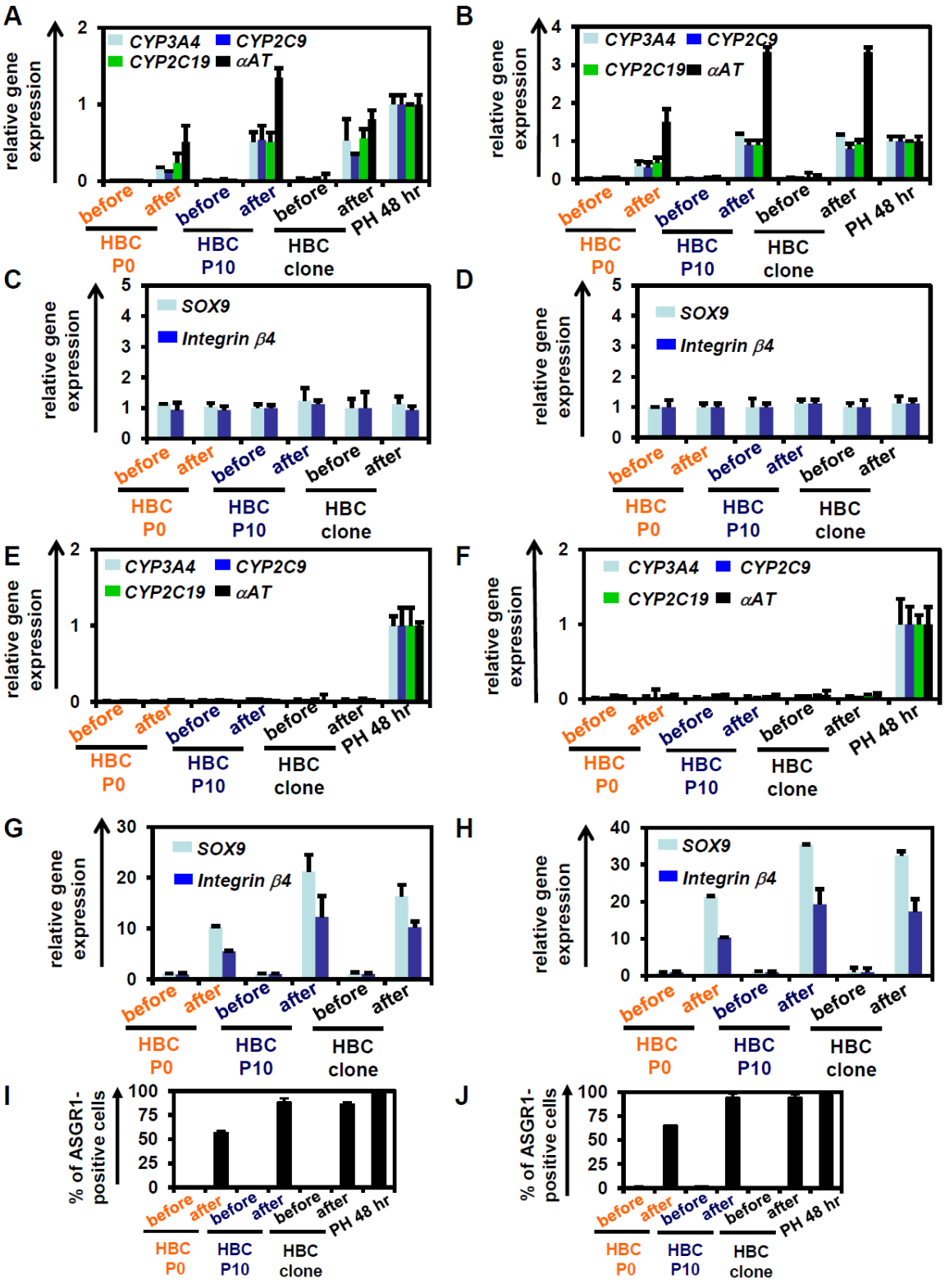

Figure S4. Hepatocyte and cholangiocyte differentiation capacity of the hESC/iPSC-derived HBCs, Related to Figure 4

(**A-D**) The hESC (H1 (**A, C**)) or hiPSC (Dotcom (**B, D**))-derived HBC P0, HBC P10, or HBC clone were differentiated into hepatocyte-like cells as described in **Figure 4A**. The gene expression levels of hepatocyte (*CYP3A4*, *2C9*, *2C19*, and *αAT*) (**A, B**) and cholangiocyte (*SOX9* and *integrin β4*) (**C, D**) markers in the HBC P0-, HBC P10-, or HBC clone-derived hepatocyte-like cells were measured by real-time RT-PCR after 14 days of differentiation. The gene expression levels of hepatocyte markers in PH 48hr were taken as 1.0 in **Figure S4A, B**. The gene expression levels of cholangiocyte markers in the hESC/hiPSC-derived HBC P10 (before hepatocyte differentiation) were taken as 1.0 in **Figure S4C, D**. Data represent the mean ± SD from three independent experiments. Student's *t* test indicated that gene expression levels of hepatocyte markers in "after" were significantly higher than those in "before" ($P<0.01$). (**E-H**) The hESC (H1 (**E, G**)) or hiPSC (Dotcom (**F, H**))-derived HBC P0, HBC P10, or HBC clone were differentiated into cholangiocyte-like cells as described in **Figure 4H**. The gene expression levels of hepatocyte (*CYP3A4*, *2C9*, *2C19*, and *αAT*) (**E, F**) and cholangiocyte (*SOX9* and *integrin β4*) (**G, H**) markers in the HBC P0-, HBC P10-, or HBC clone-derived cholangiocyte-like cells were measured by real-time RT-PCR after 14 days of differentiation. The gene expression levels of hepatocyte markers in PH 48hr were taken as 1.0 in **Figure S4E, F**. The gene expression levels of cholangiocyte markers in the hESC/hiPSC-derived HBC P10 (before cholangiocyte differentiation) were taken as 1.0 in **Figure S4G, H**. Data represent the mean ± SD from three independent experiments. Student's *t* test indicated that gene expression levels of cholangiocyte markers in "after" were significantly higher than those in "before" ($P<0.01$). (**I, J**) The efficiency of hepatocyte differentiation from the hESC (H1 (**I**)) or hiPSC (Dotcom (**J**))-derived HBC P0, HBC P10, or HBC clone was measured by estimating the percentage of ASGR1-positive cells using FACS analysis. Data represent the mean ± SD from three independent experiments. Student's *t* test indicated that percentage of ASGR1-postive cells in "after" were significantly higher than those in "before" ($P<0.01$). "Before" indicated the HBCs before hepatocyte or cholangiocyte differentiation; "After" indicated the HBCs after hepatocyte or cholangiocyte differentiation.

Supplemental figure 5

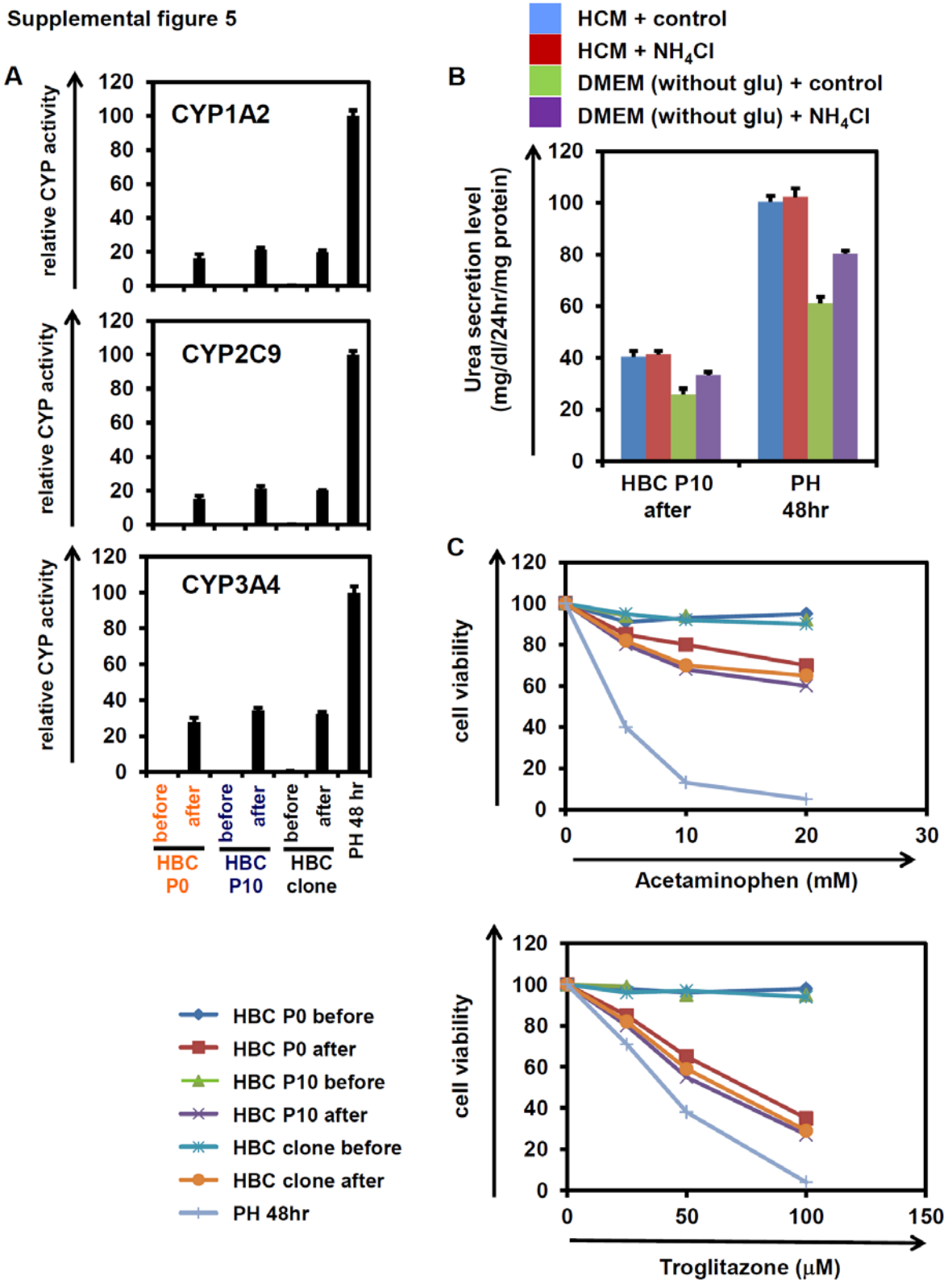

Figure S5. CYP metabolism capacity, urea production ability, potential of drug screening application of the hESC-derived HBCs, Related to Figure 4

(**A**) The hESC (H9)-derived HBC P0, HBC P10, or HBC clone were differentiated into hepatocyte-like cells as described in **Figure 4A**. The CYP1A2, 2C9, and 3A4 activity levels were measured after 14 days of hepatocyte differentiation. The CYP activity levels in PH 48hr were taken as 100. Data represent the mean ± SD from three independent experiments. Student's *t* test indicated that the CYP activity in "after" were significantly higher than those in "before" ($P<0.01$). (**B**) The hESC (H9)-derived HBC P10 were differentiated into hepatocyte-like cells as described in **Figure 4A**. After 14 days of hepatocyte differentiation, the HBC-derived hepatocyte-like cells were cultured in HCM (contains glutamine) or DMEM (do not contain glutamine) in the presence or absence of 1 mM ammonium chloride (NH_4Cl) for 24 hr, and then the amount of urea secretion was measured. PH 48hr were also cultured in HCM (containing glutamine) or DMEM (not containing glutamine) in the presence or absence of 1 mM ammonium chloride (NH_4Cl) for 24 hr, and then the amount of urea secretion was measured. Data represent the mean ± SD from three independent experiments. Student's *t* test indicated that the urea secretion levels in the "DMEM (without glu) + NH_4Cl" were significantly higher than those in the "DMEM (without glu) + control" ($P<0.05$). (**C**) The cell viability of HBC P0 before, HBC P0 after, HBC P10 before, HBC P10 after, HBC clone before, HBC clone after, and PH 48hr was assessed by WST-8 assay after 48 hr exposure to different concentrations of acetaminophen and troglitazone. The susceptibility of the HBC was higher than that of the HBC before. The cell viability was expressed as a percentage of that in the cells treated only with solvent. These data are representative of two independent experiments. "Before" indicated the HBCs before hepatocyte or cholangiocyte differentiation; "After" indicated the HBCs after hepatocyte or cholangiocyte differentiation.

Table S1. The colony formation capacity of the hESC-derived HBCs on various laminins was examined, Related to Figure 4

human reconbinant laminin	ALB+ / CK7+	ALB+ / CK7-	ALB- / CK7+
LN111	12	0	0
LN211	6	1	2
LN411	1	3	26
LN511	2	5	25

The colonies were separated into three groups based on the expression of albumin and CK7. The numbers represent total colony counts in ten 96-well plates. At 7 days after plating, the cells were fixed in 4% paraformaldehyde and used for double immunostaining. Data are representative of three independent experiments. The efficacy of the cloning on human LN11-coated dishes was approximately 0.1%.

Table S2. The primary antibodies used in this study, Related to Figures 1–5

antigen	type	company
Alpha-1-fetoprotein	rabbit	DAKO
integrin α6	mouse	BioLegend
integrin β1 (for inhibition assay)	mouse	abcam
integrin β1 (for FACS)	rabbit	Bethyl Laboratories
CK7	mouse	Invitrogen
CK19	mouse	Invitrogen
ALB	goat	Bethyl Laboratories
CYP3A4	goat	Santa Cruz Biotechnology
ASGR1	goat	Santa Cruz Biotechnology
αAT	rabbit	DAKO
HNF4α	goat	Santa Cruz Biotechnology
control IgG	rabbit	Santa Cruz Biotechnology
control IgG	mouse	Santa Cruz Biotechnology
control IgG	goat	Santa Cruz Biotechnology

Table S3. The secondary antibodies used in this study, Related to Figures 1–5

antigen	type	company
rabbit IgG	alexa fluor 594	Molecular Probes
rabbit IgG	alexa fluor 488	Molecular Probes
mouse IgG	alexa fluor 594	Molecular Probes
mouse IgG	alexa fluor 488	Molecular Probes
goat IgG	alexa fluor 594	Molecular Probes
goat IgG	alexa fluor 488	Molecular Probes

Table S4. The primers used for real-time RT-PCR in this study, Related to Figures 1, 3, and 4

Gene Symbol	Primers (forward/reverse; 5' to 3')
AFP	TGGGACCCGAACTTTCCA/GGCCACATCCAGGACTAGTTTC
ALB	GCACAGAATCCTTGGTGAACAG/ATGGAAGGTGAATGTTTTCAGCA
CD13	GACCAAAGTAAAGCGTGGAATCG/TCTCAGCGTCACCCGGTAG
CD133	AGTCGGAAACTGGCAGATAGC/GGTAGTGTTGTACTGGGCCAAT
CK18	GGGCCCAATATGACGAGCTG/AGCAGGATCCCGTTGAGCTG
CK19	CTCCCGCGACTACAGCCACT/TCAGCTCATCCAGCACCCTG
CK7	AGACGGAGTTGACAGAGCTG/GGATGGCCCGGTTCATCTC
CK8	TGAGGTCAAGGCACAGTACG/TGATGTTCCGGTTCATCTCA
claudin 3	AACACCATTATCCGGGACTTCT/GCGGAGTAGACGACCTTGG
CYP2C19	ACTTGGAGCTGGGACAGAGA/CATCTGTGTAGGGCATGTGG
CYP2C9	GGACAGAGACGACAAGCACA/CATCTGTGTAGGGCATGTGG
CYP3A4	AGATGCCTTTAGGTCCAATGGG/GCTGGAGATAGCAATGTTCGT
CYP3A7	AAGGTCGCCTCAAAGAGACA/TGCACTTTCTGCTGGACATC
CYP7A1	GAGAAGGCAAACGGGTGAAC/GCACAACACCTTATGGTATGACA
DLK1	AGCATTCATAGAGGCCATCG/CAGTGCATTTGCACCGAC
EpCAM	AATCGTCAATGCCAGTGTACTT/TCTCATCGCAGTCAGGATCATAA
GAPDH	GGTGGTCTCCTCTGACTTCAACA/GTGGTCGTTGAGGGCAATG
GATA4	CATCAAGACGGAGCCTGGCC/TGACTGTCGGCCAAGACCAG
GATA6	CCATGACTCCAACTTCCACC/ACGGAGGACGTGACTTCGGC
GSC	TCTCAACCAGCTGCACTGTC/CGTTCTCCGACTCCTCTGAT
I-CAM	ATGCCCAGACATCTGTGTCC/GGGGTCTCTATGCCCAACAA
integrin α1	CCAAACATGTCTTCCACCG/CTGCTGCTGGCTCCTCAC
integrin α2	TCACTTGAAGGACCGGAAAA/CTGGTGTTAGCGCTCAGTCA
integrin α3	GGTTGGTGTAGCCATCGG/CCTCTTCGGCTACTCGGTC
integrin α4	TGGCTGTCTGGAAAGTGTGA/AGACGTGCGAACAGCTCC
integrin α5	AGGTAGACAGCACCACCCTG/CTCAGTGGAGTTTTACCGGC
integrin α6	GTTGGCTCTCTGCAGTGGAA/CCTCTTCGGCTTCTCGCT
integrin α9	TGTAGGCTGCTTCAAACACG/GCTGCAGCTGACTTACATGG
integrin αv	TCCAAACCACTGATGGGACT/GTGACTGGTCTTCTACCCGC
integrin β1	CCTACTTCTGCACGATGTGATG/CCTTTGCTACGGTTGGTTACATT

integrin β3	GTGACCTGAAGGAGAATCTGC/CCGGAGTGCAATCCTCTGG
integrin β4	GCAGCTTCCAAATCACAGAGG/CCAGATCATCGGACATGGAGTT
MIXL1	CCGAGTCCAGGATCCAGGTA/CTCTGACGCCGAGACTTGG
NANOG	AGAAGGCCTCAGCACCTAC/GGCCTGATTGTTCCAGGATT
N-CAM	GGCATTTACAAGTGTGTGGTTAC/TTGGCGCATTCTTGAACATGA
OCT3/4	CTTGAATCCCGAATGGAAAGGG/GTGTATATCCCAGGGTGATCCTC
PROX1	TTGACATTGGAGTGAAAAGGACG/TGCTCAGAACCTTGGGGATTC
SOX17	GTGGACCGCACGGAATTTG/GAGGCCCATCTCAGGCTTG
SOX2	GGCAGCTACAGCATGATGATGCAGGAGC/CTGGTCATGGAGTTGTACTGCAGG
SOX9	TTTCCAAGACACAAACATGA/AAAGTCCAGTTTCTCGTTGA
T	TGCTTCCCTGAGACCCAGTT/GATCACTTCTTTCCTTTGCATCAAG
TO	GGCAGCGAAGAAGACAAATC/TCGAACAGAATCCAACTCCC
αAT	ACTGTCAACTTCGGGGACAC/CATGCCTAAACGCTTCATCA

Table S5. The amplification efficacy of beta integrin beta1, beta3, and beta4 primers, Related to Figure 1

	slope	e
ITGB1	-3.367	0.981528
ITGB3	-3.369	0.980724
ITGB4	-3.36	0.984354

Supplemental References

Schmelzer, E., Zhang, L., Bruce, A., Wauthier, E., Ludlow, J., Yao, H.L., Moss, N., Melhem, A., McClelland, R., Turner, W., et al. (2007). Human hepatic stem cells from fetal and postnatal donors. J Exp Med *204*, 1973-1987.

Zhang, L., Theise, N., Chua, M., and Reid, L.M. (2008). The stem cell niche of human livers: symmetry between development and regeneration. Hepatology *48*, 1598-1607.